

PACS: 546.882

ISSN 1729-4428

L. Romaka<sup>1</sup>, I. Romaniv<sup>1</sup>, V.V. Romaka<sup>2</sup>, M. Konyk<sup>1</sup>, A. Horyn<sup>1</sup>, Yu. Stadnyk<sup>1</sup>

## Isothermal Section of the Ho–Cu–Sn Ternary System at 670 K

<sup>1</sup>*Inorganic Chemistry Department, Ivan Franko Lviv National University, Kyryla and Mefodiya str. 6, 79005 Lviv, Ukraine*

<sup>2</sup>*Department of Materials Engineering and Applied Physics, Lviv Polytechnic National University, Ustyianovycha Str. 5, 79013, Lviv, Ukraine*

The interaction of the components in the Ho–Cu–Sn ternary system was investigated at 670 K over the whole concentration range using X-ray diffraction and EPM analyses. Four ternary compounds were formed in the Ho–Cu–Sn system at 670 K: HoCuSn (LiGaGe type, space group  $P6_3mc$ ),  $Ho_3Cu_4Sn_4$  (Gd<sub>3</sub>Cu<sub>4</sub>Ge<sub>4</sub>-type, space group  $Imm\bar{m}$ ), HoCu<sub>5</sub>Sn (CeCu<sub>5</sub>Au-type, space group  $Pnma$ ), and  $Ho_{1.9}Cu_{9.2}Sn_{2.8}$  (Dy<sub>1.9</sub>Cu<sub>9.2</sub>Sn<sub>2.8</sub>-type, space group  $P6_3/mmc$ ). The formation of the interstitial solid solution based on HoSn<sub>2</sub> (ZrSi<sub>2</sub>-type) binary compound up to 5 at. % Cu was found.

**Keywords:** Intermetallics; Phase diagrams; X-ray diffraction; Crystal structure.

Article acted received 22.05.2018; accepted for publication 15.06.2018.

## Introduction

Among R–M–Sn systems (R- rare earth element, M- d-element) the ternary systems with rare earth metals, copper and tin were studied with the most rare earths [1–14] and are characterized by a large variety of stoichiometry and crystal structures of the intermediate ternary phases. An analysis of previously studied R–Cu–Sn systems with light rare earths and heavy rare earth elements indicated the significant influence of f-element on the formation, chemical and structural characteristics of intermediate ternary phases. The RCu<sub>1-x</sub>Sn<sub>x</sub> (CeNiSi<sub>2</sub>-type) and RCu<sub>9</sub>Sn<sub>4</sub> (LaFe<sub>9</sub>Si<sub>4</sub>-type) [15, 16] compounds are typical for the light rare-earth containing systems, while the stannides RCuSn (LiGaGe-type, CeCu<sub>2</sub>-type (Eu, Yb), AlB<sub>2</sub>-type (La)), R<sub>3</sub>Cu<sub>4</sub>Sn<sub>4</sub> (Gd<sub>3</sub>Cu<sub>4</sub>Ge<sub>4</sub>-type), R<sub>1.9</sub>Cu<sub>9.2</sub>Sn<sub>2.8</sub> (Dy<sub>1.9</sub>Cu<sub>9.2</sub>Sn<sub>2.8</sub>-type) and RCu<sub>5</sub>Sn (CeCu<sub>5</sub>Au-, CeCu<sub>6</sub> structure types) were realized with the most rare earths [17, 18]. Previous investigations of the R–Cu–Sn ternary systems with rare earths of Yttrium group (R = Y, Gd, Dy, Er, Lu) [1, 9–11, 14] showed the quite decreasing number of formed compounds up to three for the Lu–Cu–Sn system, excepting the Yb–Cu–Sn system where ten intermediate phases were found at 673 K [13]. In case of Yb the structure and stoichiometry of several compounds differ from other rare earths: Yb<sub>3</sub>Cu<sub>6</sub>Sn<sub>5</sub> (Dy<sub>3</sub>Co<sub>6</sub>Sn<sub>5</sub>-type), Yb<sub>3</sub>Cu<sub>8</sub>Sn<sub>4</sub> (Lu<sub>3</sub>Co<sub>7.77</sub>Sn<sub>4</sub>-type), Yb<sub>5</sub>Cu<sub>11</sub>Sn<sub>8</sub> (own structure type) [19], Yb<sub>4</sub>Cu<sub>2</sub>Sn<sub>5</sub> (own structure type) [20]. In the Cu-rich corner of R–Cu–Sn systems the

formation of the RCu<sub>5</sub>Sn compounds (except “LuCu<sub>5</sub>Sn” phase in the Lu–Cu–Sn system) and R<sub>1.9</sub>Cu<sub>9.2</sub>Sn<sub>2.8</sub> (R=Y, Ce–Nd, Sm, Gd–Lu) was observed. The structures of the both phases are derivative of the hexagonal CaCu<sub>5</sub> structure type [21, 22].

In the present paper the results of X-ray and EPM analyses of the phase equilibria in the Ho–Cu–Sn system at 670 K and crystallographic data of the ternary compounds are reported. The data concerning the Ho–Sn binary system were taken from Refs. [23–27], those of the Ho–Cu and Cu–Sn systems were found in Refs [28, 29].

## I. Experimental details

The samples were prepared by a direct twofold arc melting of the constituent metals (holmium, purity of 99.9 wt.%; copper, purity of 99.99 wt.%; and tin, purity of 99.999 wt.%) under high purity Ti-gettered argon atmosphere on a water-cooled copper crucible. The weight losses of the initial total mass were lower than 1 wt.%. The pieces of the as-cast buttons were annealed for one month at 670 K in evacuated silica tubes and then water quenched. The temperature of annealing was chosen taking into account the low melting temperature of Sn (232 °C) and of the R–Sn binaries at high Sn content. Phase analysis was performed using X-ray powder patterns of the synthesized and annealed samples (DRON-2.0, Fe  $K_\alpha$  radiation). The observed diffraction

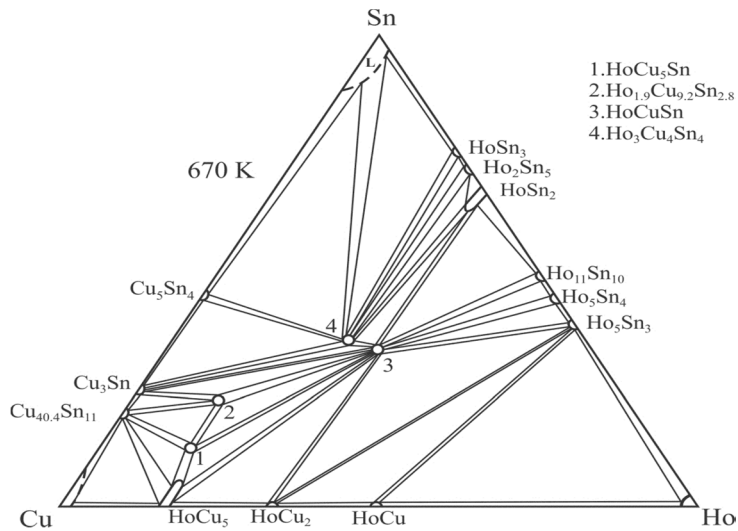


**Fig. 1.** Isothermal section of the Ho–Cu–Sn system at 670 K.

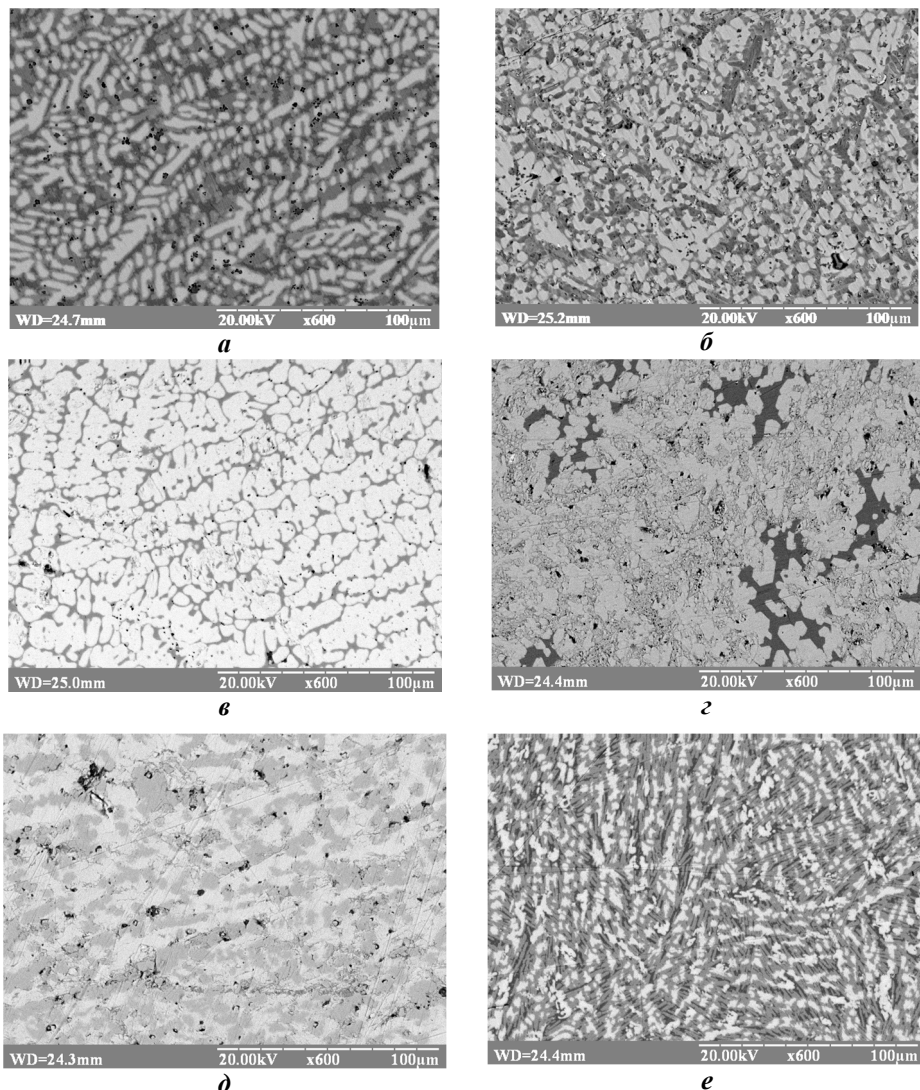


**Fig. 2.** SEM pictures of the alloys from Ho–Cu–Sn system (the alloys are numbered according to Table 1): a) 4. Ho<sub>30</sub>Cu<sub>55</sub>Sn<sub>15</sub> (HoCuSn—grey light phase, HoCu<sub>5-x</sub>Sn<sub>x</sub>—grey phase, HoCu<sub>2</sub>—dark phase); b) 5. Ho<sub>40</sub>Cu<sub>40</sub>Sn<sub>20</sub> (HoCuSn—light phase, Ho<sub>5</sub>Sn<sub>3</sub>—grey phase, HoCu<sub>2</sub>—dark phase); c) 7. Ho<sub>30</sub>Cu<sub>44</sub>Sn<sub>26</sub> (HoCuSn—light phase, HoCu<sub>5-x</sub>Sn<sub>x</sub>—dark phase); d) 13. Ho<sub>20</sub>Cu<sub>33</sub>Sn<sub>47</sub> (Ho<sub>3</sub>Cu<sub>4</sub>Sn<sub>4</sub>—light phase, Cu<sub>5</sub>Sn<sub>4</sub>—grey phase, Sn—dark phase); e) 14. Ho<sub>30</sub>Cu<sub>15</sub>Sn<sub>55</sub> (Ho<sub>3</sub>Cu<sub>4</sub>Sn<sub>4</sub>—grey phase, HoSn<sub>2</sub>—light phase, Ho<sub>11</sub>Sn<sub>10</sub>—dark phase); f) 6. Ho<sub>15</sub>Cu<sub>60</sub>Sn<sub>25</sub> (Ho<sub>1.9</sub>Cu<sub>9.2</sub>Sn<sub>2.8</sub>—grey phase, HoCuSn—grey light phase, Cu<sub>3</sub>Sn—dark phase).

## Isothermal Section of the Ho–Cu–Sn Ternary System at 670 K

Table 1

Phase composition of the selected Ho–Cu–Sn alloys

N	Nominal alloy composition (at.%)			Phases		
	Ho	Cu	Sn	1 <sup>st</sup> phase	2 <sup>nd</sup> phase	3 <sup>rd</sup> phase
1	17	78	5	HoCu <sub>5-x</sub> Sn <sub>x</sub> <i>a</i> = 0.7048(2) nm		
2	40	53	7	HoCu <sub>2</sub> <i>a</i> = 0.4277(4) nm <i>b</i> = 0.6758(3) nm <i>c</i> = 0.7269(5) nm	HoCu <i>a</i> = 0.3444(3) nm	Ho <sub>5</sub> Sn <sub>3</sub> <i>a</i> = 0.8844(4) nm <i>c</i> = 0.6452(4) nm
3	17	68	15	HoCu <sub>5</sub> Sn <i>a</i> = 0.8189(4) nm <i>b</i> = 0.4960(4) nm <i>c</i> = 1.0568(6) nm	Ho <sub>1.9</sub> Cu <sub>9.2</sub> Sn <sub>2.8</sub> <i>a</i> = 0.5055(4) nm <i>c</i> = 2.0580(6) nm	HoCuSn <i>a</i> = 0.4470(3) nm <i>c</i> = 0.7155(5) nm
4	30	55	15	HoCuSn <i>a</i> = 0.4471(3) nm <i>c</i> = 0.7153(5) nm	HoCu <sub>5-x</sub> Sn <sub>x</sub> <i>a</i> = 0.7038(3) nm	HoCu <sub>2</sub> <i>a</i> = 0.4277(3) nm <i>b</i> = 0.6759(4) nm <i>c</i> = 0.7270(5) nm
5	40	40	20	HoCuSn <i>a</i> = 0.4472(3) nm <i>c</i> = 0.7153(4) nm	Ho <sub>5</sub> Sn <sub>3</sub> <i>a</i> = 0.8843(4) nm <i>c</i> = 0.6453(3) nm	HoCu <sub>2</sub> <i>a</i> = 0.4278(4) nm <i>b</i> = 0.6757(5) nm <i>c</i> = 0.7270(5) nm
6	15	65	25	Ho <sub>1.9</sub> Cu <sub>9.2</sub> Sn <sub>2.8</sub> <i>a</i> = 0.5054(3) nm <i>c</i> = 2.0580(5) nm	HoCuSn <i>a</i> = 0.4470(3) nm <i>c</i> = 0.7153(4) nm	Cu <sub>3</sub> Sn (not determined)
7	30	44	26	HoCuSn <i>a</i> = 0.4470(3) nm <i>c</i> = 0.7152(3) nm	HoCu <sub>5-x</sub> Sn <sub>x</sub> <i>a</i> = 0.7047(2) nm	
8	25	55	20	HoCuSn <i>a</i> = 0.4473(3) nm <i>c</i> = 0.7155(3) nm	HoCu <sub>5</sub> <i>a</i> = 0.7046(2) nm	HoCu <sub>5</sub> Sn (traces)
9	15	55	30	Ho <sub>3</sub> Cu <sub>4</sub> Sn <sub>4</sub> <i>a</i> = 0.4421(3) nm <i>b</i> = 0.6940(6) nm <i>c</i> = 1.4549(8) nm	Cu <sub>3</sub> Sn <i>a</i> = 0.4317(3) nm <i>b</i> = 0.5486(4) nm <i>c</i> = 0.4737(4) nm	HoCuSn (traces)
10	50	13	37	HoCuSn <i>a</i> = 0.4470(3) nm <i>c</i> = 0.7154(4) nm	Ho <sub>5</sub> Sn <sub>3</sub> <i>a</i> = 0.8845(4) nm <i>c</i> = 0.6457(4) nm	Ho <sub>5</sub> Sn <sub>4</sub> <i>a</i> = 0.7961(4) nm <i>b</i> = 1.5300(7) nm <i>c</i> = 0.8053(4) nm
11	12	50	38	Ho <sub>3</sub> Cu <sub>4</sub> Sn <sub>4</sub> <i>a</i> = 0.4420(4) nm <i>b</i> = 0.6936(5) nm <i>c</i> = 1.4548(8) nm	Cu <sub>5</sub> Sn <sub>4</sub> <i>a</i> = 1.1015(6) nm <i>b</i> = 0.7273(4) nm <i>c</i> = 0.9817(5) nm <i>b</i> = 98.79	Cu <sub>3</sub> Sn (traces)
12	45	10	45	HoCuSn <i>a</i> = 0.4471(3) nm <i>c</i> = 0.7153(5) nm	Ho <sub>11</sub> Sn <sub>10</sub> <i>a</i> = 1.1519(5) nm <i>c</i> = 1.6788(5) nm	
13	20	33	47	Ho <sub>3</sub> Cu <sub>4</sub> Sn <sub>4</sub> <i>a</i> = 0.4419(3) nm <i>b</i> = 0.6938(6) nm <i>c</i> = 1.4545(8) nm	Cu <sub>5</sub> Sn <sub>4</sub> <i>a</i> = 1.1014(7) nm <i>b</i> = 0.7274(4) nm <i>c</i> = 0.9819(6) nm <i>b</i> = 98.81(1)	Sn <i>a</i> = 0.5808(4) nm <i>c</i> = 0.3177(5) nm
14	40	10	50	HoCuSn <i>a</i> = 0.4474(2) nm <i>c</i> = 0.7156(3) nm	HoSn <sub>2</sub> <i>a</i> = 0.4389(3) nm <i>b</i> = 1.6188(5) nm <i>c</i> = 0.4294(4) nm	Ho <sub>11</sub> Sn <sub>10</sub> (traces)
15	30	15	55	Ho <sub>3</sub> Cu <sub>4</sub> Sn <sub>4</sub> <i>a</i> = 0.4419(3) nm <i>b</i> = 0.6938(6) nm <i>c</i> = 1.4547(8) nm	HoSn <sub>2</sub> <i>a</i> = 0.4393(3) nm <i>b</i> = 1.6193(5) nm <i>c</i> = 0.4297(4) nm	

**Table 2**

Crystallographic characteristics of the Ho-Sn binary phases (670 K)

Compound	Space group	Structure type	Lattice parameters, nm		
			<i>a</i>	<i>b</i>	<i>c</i>
HoSn <sub>3</sub>	<i>Amm2</i>	GdSn <sub>2.75</sub>	0.4338(3)	0.4389(3)	2.1756(7)
Ho <sub>2</sub> Sn <sub>5</sub>	<i>Pmmn</i>	Er <sub>2</sub> Ge <sub>5</sub>	0.4305(1)	0.4385(5)	1.8903(1)
HoSn <sub>2</sub>	<i>Cmcm</i>	ZrSi <sub>2</sub>	0.4382(2)	1.6193(3)	0.4290(2)
Ho <sub>11</sub> Sn <sub>10</sub>	<i>I4/mmm</i>	Ho <sub>11</sub> Ge <sub>10</sub>	1.1526(5)		1.6768(6)
Ho <sub>5</sub> Sn <sub>4</sub>	<i>Pnma</i>	Sm <sub>5</sub> Ge <sub>4</sub>	0.7963(3)	1.5302(5)	0.8053(2)
Ho <sub>5</sub> Sn <sub>3</sub>	<i>P6<sub>3</sub>/mcm</i>	Mn <sub>5</sub> Si <sub>3</sub>	0.8846(2)		0.6453(3)

**Table 3**

Crystallographic characteristics of the ternary compounds in the Ho-Cu-Sn system

Compound	Space group	Structure type	Lattice parameter, nm		
			<i>a</i>	<i>b</i>	<i>c</i>
HoCu <sub>5</sub> Sn	<i>Pnma</i>	CeCu <sub>5</sub> Au	0.81889(7)	0.49599(4)	0.50652(8)
Ho <sub>1.9</sub> Cu <sub>9.2</sub> Sn <sub>2.8</sub>	<i>P6<sub>3</sub>/mmc</i>	Dy <sub>1.9</sub> Cu <sub>9.2</sub> Sn <sub>2.8</sub>	0.5056(3)	-	2.0581(6)
HoCuSn	<i>P6<sub>3</sub>mc</i>	LiGaGe	0.4474(2)	-	0.7155(3)
Ho <sub>3</sub> Cu <sub>4</sub> Sn <sub>4</sub>	<i>Immm</i>	Gd <sub>3</sub> Cu <sub>4</sub> Ge <sub>4</sub>	0.44197(1)	0.69065(1)	1.45799(3)

**Table 4**Atomic positional and isotropic displacement parameters of the HoCu<sub>5</sub>Sn compound ( $R_p = 0.0358$ ,  $R_{wp} = 0.0565$ ,  $R_I = 0.0448$ )

Atom	Wyckoff position	<i>x/a</i>	<i>y/b</i>	<i>z/c</i>	$B_{iso} \cdot 10^2$ (nm <sup>2</sup> )
Ho	4c	0.2530(2)	0.25	0.5630(1)	1.49(3)
Cu1	8d	0.0688(2)	0.4997(3)	0.3110(2)	1.07(4)
Cu2	4c	0.0597(3)	0.25	0.0977(3)	1.25(5)
Cu3	4c	0.3190(3)	0.25	0.2410(2)	1.16(6)
Cu4	4c	0.4162(3)	0.25	0.0143(2)	1.15(6)
Sn	4c	0.1386(2)	0.25	0.8605(1)	0.88(2)

intensities were compared with reference powder patterns of the binary and known ternary phases. The chemical and phase compositions of the samples were examined by Scanning Electron Microscopy (SEM) using REMMA-102-02 scanning microscope. Quantitative electron probe microanalysis (EPMA) of the samples was carried out by using an energy-dispersive X-ray analyzer with the pure elements as standards (an acceleration voltage was 20 kV; *K*- and *L*-lines were used). XRPD data were collected in the transmission mode on a STOE STADI P diffractometer (linear PSD detector,  $2q/\omega$ -scan; Cu  $K\alpha_1$  radiation, curved germanium (1 1 1) monochromator). Calculations of the crystallographic parameters were performed using WinCSD and WinPLOTR program packages [30, 31].

The DSC analysis was performed on the Ho<sub>3</sub>Cu<sub>4</sub>Sn<sub>4</sub> compound (LINSEIS STA PT 1600 device, argon atmosphere). The Ho<sub>3</sub>Cu<sub>4</sub>Sn<sub>4</sub> sample was heated up to 1023 K and cooled down to room temperature at a rate of 10 K/min. The weight losses during heating (TG) were negligible (less than 0.3%).

## II. Results

### 2.1. Isothermal section of the Ho-Cu-Sn system.

Phase equilibria in the Ho-Cu-Sn system have been studied using X-ray analysis and scanning electron microscopy of 15 binary and 29 ternary alloys annealed at 670 K (Fig. 1). The phase compositions of the selected samples are listed in Table 1, the SEM-pictures of some alloys are shown in Fig. 2.

The presence of the all binary compounds in the Ho-Cu and Cu-Sn systems corresponding to the reference data was confirmed at 670 K. Taking into account the reported data on Ho-Sn system including experimental study and thermodynamic optimization, and previously known binaries [23-27], the samples with compositions corresponding to the reference data were synthesized and analyzed by X-ray powder diffraction. The performed analysis confirmed the formation of Ho<sub>5</sub>Sn<sub>3</sub> (Mn<sub>5</sub>Si<sub>3</sub>-type), Ho<sub>5</sub>Sn<sub>4</sub> (Sm<sub>5</sub>Ge<sub>4</sub>-type), Ho<sub>11</sub>Sn<sub>10</sub> (Ho<sub>11</sub>Ge<sub>10</sub>-type), HoSn<sub>2</sub> (ZrSi<sub>2</sub>-type), Ho<sub>2</sub>Sn<sub>5</sub> (Er<sub>2</sub>Ge<sub>5</sub>-type) and HoSn<sub>3</sub> (GdSn<sub>2.75</sub>-type) binaries. However, two binaries Ho<sub>4</sub>Sn<sub>5</sub> and Ho<sub>3</sub>Sn<sub>7</sub> were not identified at temperature of annealing, corresponding samples contained only

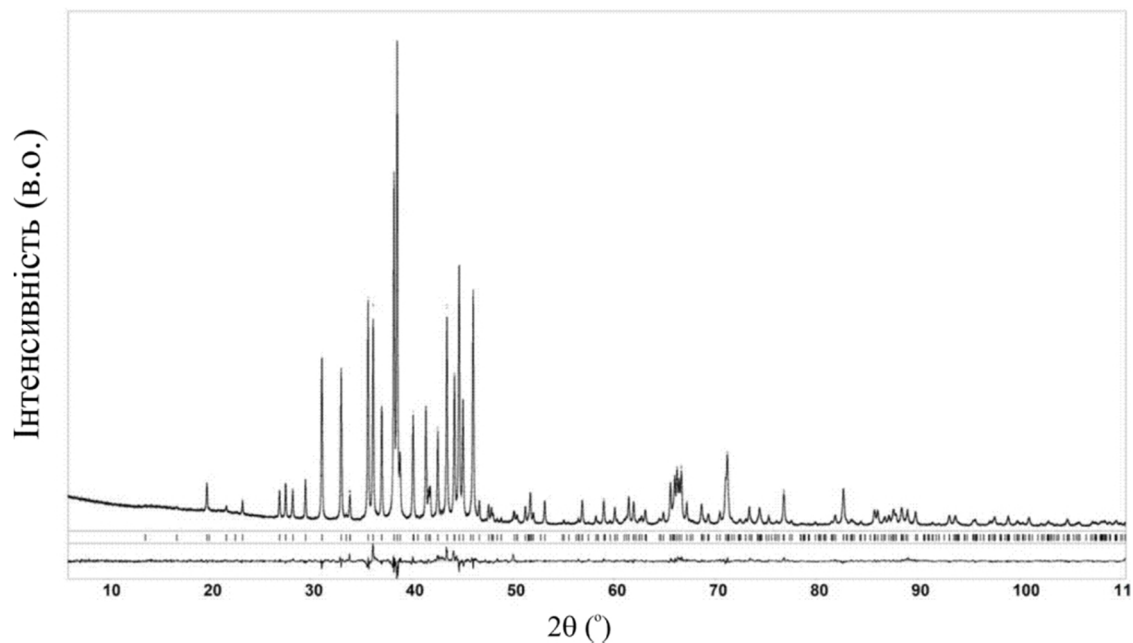


**Fig. 3.** The observed, calculated and difference X-ray patterns of  $\text{HoCu}_5\text{Sn}$  compound.

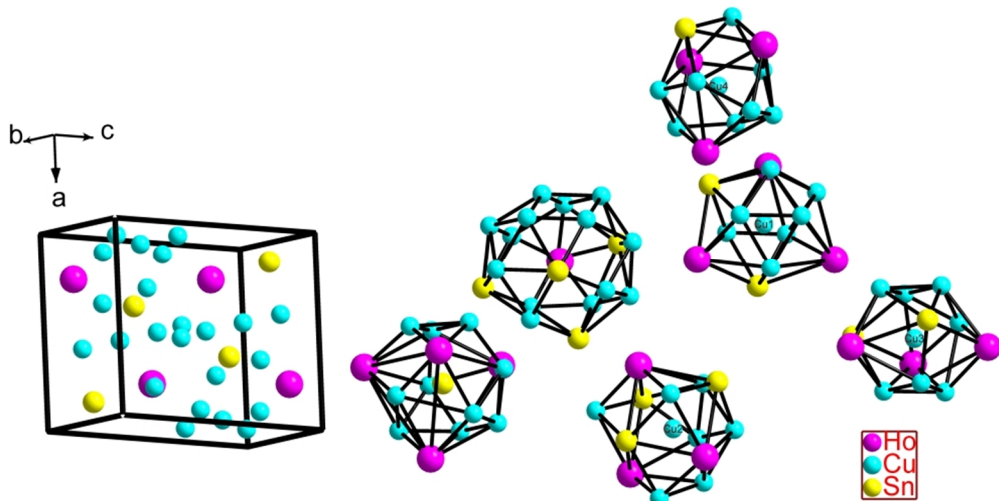


**Fig. 4.** Crystal structure model of the  $\text{HoCu}_5\text{Sn}$  compound.

$\text{Ho}_{11}\text{Sn}_{10}$ ,  $\text{HoSn}_2$  and  $\text{Ho}_2\text{Sn}_5$ ,  $\text{HoSn}_2$  phases, respectively. Obtained results are in agreement with last version of Ho–Sn phase diagram [27]. Crystallographic characteristic of the Ho–Sn binary compounds are given in Table 2. The formation of the substitutional solid solution based on the  $\text{HoCu}_5$  binary compound (AuBe<sub>5</sub>-type) up to 5 at.% Sn was found ( $a = 0.7028(2)$  nm for  $\text{HoCu}_5$ ,  $a = 0.7048(2)$  nm for  $\text{Ho}_{17}\text{Cu}_{78}\text{Sn}_5$ ). The limiting composition was confirmed by EPMA data ( $\text{Ho}_{17.62}\text{Cu}_{77.55}\text{Sn}_{4.83}$ , Fig. 2a). The interstitial solid solution  $\text{HoCu}_x\text{Sn}_2$  (up to 6 at.% Cu) based on the  $\text{HoSn}_2$  (ZrSi<sub>2</sub>-type) binary compound was observed similarly to Ref. [32] ( $a = 0.4393(3)$ ,  $b = 1.6197(5)$ ,  $c = 0.4298(4)$  nm for  $\text{Ho}_{31/5}\text{Cu}_5\text{Sn}_{63/5}$ ). No significant solubility of the third component in the other binary compounds was observed under used in our work conditions.

According to performed X-ray and microprobe analyses the phase relations in the Ho–Cu–Sn system at 670 K are characterized by the formation of four ternary

compounds listed in Table 3. All ternary compounds are characterized by narrow homogeneity regions at investigated temperature. Among formed ternary compounds  $\text{Ho}_3\text{Cu}_4\text{Sn}_4$  contains the higher Sn content (36 at. %), and we checked this phase with the differential scanning calorimetric analysis (DSC). No thermal peak corresponding to decomposition of  $\text{Ho}_3\text{Cu}_4\text{Sn}_4$  compound was observed on DSC curve up to 1023 K.

## 2.2. Crystal structure.

The existence of the  $\text{HoCu}_5\text{Sn}$  compound with CeCu<sub>6</sub> structure type and its lattice parameters were reported earlier [21]. In our work the crystal structure of  $\text{HoCu}_5\text{Sn}$  stannide was refined by X-ray powder diffraction method (STOE STADI P diffractometer, WinCSD program package). After Rietveld refinement it was deduced that this compound belongs to the CeCu<sub>5</sub>Au type structure (ordered variant of CeCu<sub>6</sub>-type, space group Pnma,  $a=0.81889(7)$ ,  $b=0.49599(4)$ ,  $c=0.50652(8)$

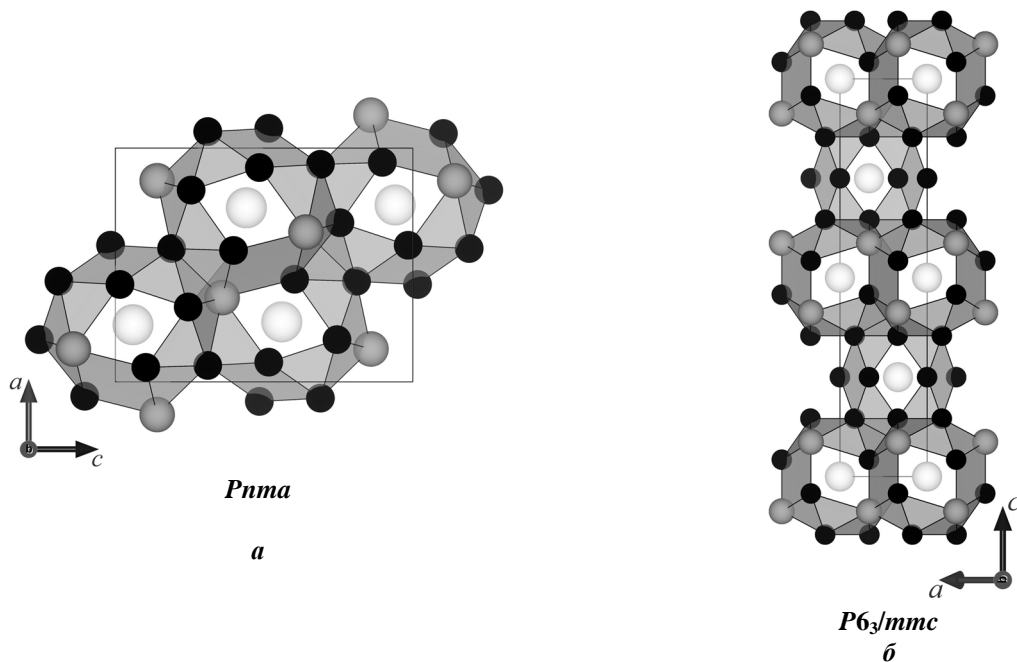


**Fig. 5.** Package of polyhydra for rare earth atoms in CeCu<sub>5</sub>Au (a) and CeNi<sub>5</sub>Sn (b) structures.

**Table 5**

Atomic positional and isotropic displacement parameters of the Ho<sub>3</sub>Cu<sub>4</sub>Sn<sub>4</sub> compound ( $R_p = 0.0856$ ,  $R_{wp} = 0.115$ ,  $R_{Bragg} = 0.0647$ )

Atom	Wyckoff position	$x/a$	$y/b$	$z/c$	$B_{iso} \cdot 10^2 (\text{nm}^2)$
Ho1	4j	1/2	0	0.3692(1)	1.25(6)
Ho2	2a	0	0	0	1.20(8)
Cu	8l	0	0.3075(4)	0.3283(2)	1.04(8)
Sn1	4i	0	0	0.2152(1)	0.59(7)
Sn2	4h	0	0.2020(3)	1/2	0.68(4)

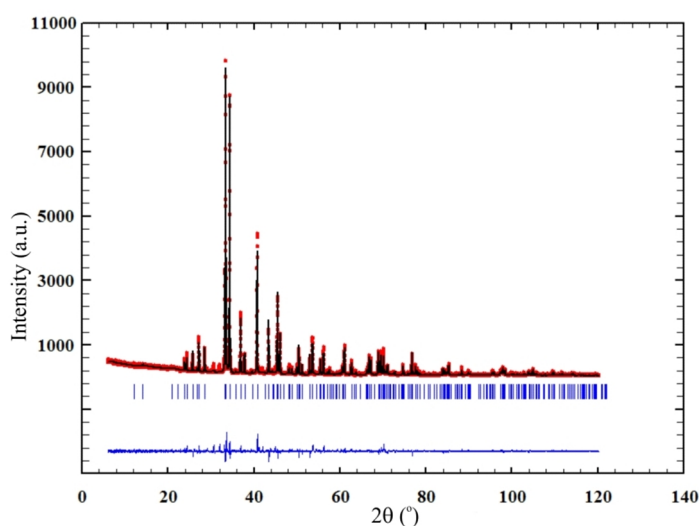


**Fig. 6.** The observed, calculated and difference X-ray patterns of Ho<sub>3</sub>Cu<sub>4</sub>Sn<sub>4</sub> compound.

nm) with ordered distribution of the all atoms. Refined atomic coordinates and displacement parameters are listed in Table 4. The observed, calculated and difference

X-ray patterns of HoCu<sub>5</sub>Sn compound are shown in Fig. 3. The interatomic distances in the HoCu<sub>5</sub>Sn structure are close to the sum of the atomic radii of the components.

Crystal structure model of the  $\text{HoCu}_5\text{Sn}$  compound is shown in Fig. 4.  $\text{CeCu}_5\text{Au}$  structure type similarly to  $\text{CeNi}_5\text{Sn}$  in which  $\text{RNi}_5\text{Sn}$  stannides with light rare earths crystallize [17], is related to  $\text{CaCu}_5$  structure. Both structures contain the fragments of  $\text{CaCu}_5$  type [33, 34]. Package of polyhydra for rare earth atoms in  $\text{CeCu}_5\text{Au}$  (a) and  $\text{CeNi}_5\text{Sn}$  (b) structures is shown in Fig. 5.

During present work, the crystal structure of  $\text{Ho}_3\text{Cu}_4\text{Sn}_4$  stannide was refined by X-ray powder diffraction method (STOE STADI P diffractometer, WinPLOTR program package). Performed calculation confirmed that  $\text{Ho}_3\text{Cu}_4\text{Sn}_4$  belongs to the  $\text{Gd}_3\text{Cu}_4\text{Ge}_4$  structure type (space group  $\text{Immm}$ ,  $a = 0.44197(1)$  nm,  $b = 0.69065(1)$  nm,  $c = 1.45799(3)$  nm). Refined atomic coordinates and displacement parameters are listed in Table 5. The observed, calculated and difference X-ray patterns of  $\text{Ho}_3\text{Cu}_4\text{Sn}_4$  compound are shown in Fig. 6.

## Final remarks

Comparing investigated Ho–Cu–Sn and previously studied R–Cu–Sn systems with heavy rare earths, it should be note a close analogy in stoichiometry and crystal structure of the most formed compounds. Similarity in the interaction of the elements in all

investigated systems is demonstrated by the formation of the compounds  $\text{RCuSn}$ ,  $\text{R}_3\text{Cu}_4\text{Sn}_4$ ,  $\text{R}_{1.9}\text{Cu}_{9.2}\text{Sn}_{2.8}$  and  $\text{RCu}_5\text{Sn}$  (except Lu). Crystal structure of the studied  $\text{HoCu}_5\text{Sn}$  compound is characterized by ordered distribution of the all atoms corresponding to  $\text{CeCu}_5\text{Au}$ -type in comparing to reported previously isotropic compound with Er ( $\text{CeCu}_6$ -type), the stoichiometry of which weakly deviates from  $\text{ErCu}_5\text{Sn}$  to  $\text{ErCu}_{4.5}\text{Sn}_{1.5}$  [21]. The equiatomic  $\text{RCuSn}$  compounds exist with all rare earths, but depending on the valence state and size of rare earth element they crystallize in different structure types -  $\text{LiGaGe}$ -type (or  $\text{CaIn}_2$ -type) (Y, La-Sm, Gd-Er, Lu) [35–38],  $\text{CeCu}_2$ -type (Eu) [39],  $\text{TiNiSi}$ -type (Yb) [40] and  $\text{ZrBeSi}$ -type (La, Ce) [35, 41]. The structure type  $\text{Sm}_2\text{Cu}_4\text{Sn}_5$  realizes in the systems with Gd, Tb and Dy. The stannides with  $\text{MgCu}_4\text{Sn}$ -type are typical for Y–Cu–Sn and Yb–Cu–Sn systems.

**Romaka L.** - Ph.D., Senior Scientist;

**Romaniv I.** - Ph.D. student;

**Romaka V.** - D.Sc., Assoc. Professor;

**Konyk M.** - Ph.D., Senior Research4

**Horyn A.** - Ph.D., Senior Research4

**Stadnyk Yu.** - Ph.D., Senior Scientist.

- [1] L. Romaka, I. Romaniv, Yu. Stadnyk, V.V. Romaka, R. Serkiz, R. Gladyshevskii, Chem. Met. Alloys 7, 132 (2014).
- [2] Y. Zhan, H. Xie, J. Jiang, Y. Xu, Y. Wang, Y. Zhuang, J. Alloys Compd. 461, 570 (2008).
- [3] P. Riani, D. Mazzone, G. Zanicchi, R. Marazza, R. Ferro, F. Faudot, M. Harmelin, J. Phase Equilibria 3, 239 (1998).
- [4] L.P. Komarovskaya, L.A. Mykhajliv, R.V. Skolozdra, Izv. AN SSSR. Metals 4, 209 (1989).
- [5] P. Riani, D. Mazzone, G. Zanicchi, R. Marazza, R. Ferro, Intermetallics 8, 259 (2000).
- [6] D. Mazzone, P.L. Paulose, S.K. Dhar, M.L. Fornasini, P. Manfrinetti, J. Alloys Compd. 453, 24 (2008).
- [7] P. Riani, D. Mazzone, G. Zanicchi, R. Marazza, J. Alloys Compd. 247, 148 (1997).
- [8] P. Riani, M.L. Fornasini, R. Marazza, D. Mazzone, G. Zanicchi, R. Ferro, Intermetallics 7, 835 (1999).
- [9] I. V. Senkovska, Ya.S. Mudryk, L.P. Romaka, O.I. Bodak, J. Alloys Compd. 312, 124 (2000).
- [10] L. Romaka, V.V. Romaka, E.K. Hlil, D. Fruchart, Chem. Met. Alloys 2(1,2), 68 (2009).
- [11] O.I. Bodak, V.V. Romaka, L.P. Romaka, A.V. Tkachuk, Yu.V. Stadnyk, J. Alloys Compd. 395, 113 (2005).
- [12] V. Romaka, Yu. Gorelenko, L. Romaka, Visnyk Lviv. Univ. Ser. Khim. 49, 3 (2008).
- [13] G. Zanicchi, D. Mazzone, M.L. Fornasini, P. Riani, R. Marazza, R. Ferro, Intermetallics 7, 957 (1999).
- [14] L. Romaka, V.V. Romaka, V. Davydov, Chem. Met. Alloys. 1(2), 192 (2008).
- [15] L.P. Komarovskaya, S.A. Sadykov, R.V. Skolozdra, Izv. AN SSSR. Metals 33(8), 1249 (1988).
- [16] S. Singh, M.L. Fornasini, P. Manfrinetti, A. Palenzona, S.K. Dhar, P.L. Paulose, J. Alloys Compd. 317-318, 560 (2001).
- [17] R.V. Skolozdra, in: K.A. Gschneidner, Jr. and L. Eyring (Eds.), Handbook on the Physics and Chemistry of Rare Earths, Vol. 24, 1997, 399 p.
- [18] V.V. Romaka, L.P. Romaka, V.Ya. Krajovskyj, Yu.V. Stadnyk, Stannides of rare earth and transition metals, Lviv Polytech. Univ. 2015, 221 p.
- [19] M.L. Fornasini, P. Manfrinetti, D. Mazzone, P. Riani, G. Zanicchi, J. Solid State Chem. 177, 1919 (2004).
- [20] M.L. Fornasini, G. Zanicchi, D. Mazzone, P. Riani, Z. Kristallogr. 216(1), 21 (2001).
- [21] Ya. Mudryk, O. Isnard, L. Romaka, D. Fruchart, Solid State Commun. 119, 423 (2001).
- [22] V.V. Romaka, D. Fruchart, R. Gladyshevskii, P. Rogl, N. Koblyuk, J. Alloys Compd. 460, 283 (2008).
- [23] A. Palenzona, P. Manfrinetti, J. Alloys Compd. 201, 43 (1993).
- [24] M.L. Fornasini, F. Merlo, G.B. Bonino, Atti Accad. Naz. Lincei 50, 186 (1971).
- [25] M.V. Bulanova, V.N. Eremenko, V.M. Petjukh, V.R. Sidorko, J. Phase Equil. 19, 136 (1998).
- [26] X.C. Zhong, M. Zou, H. Zhang, Z. W. Liu, D.C. Zeng, K.A.Jr. Gschneidner, V.K. Pecharsky, J. Appl. Phys. 109, 07A917 (2011).
- [27] J. Kim, J.-H. Jung, Calphad 55, 134 (2016).

- [28] T.B. Massalski, in: *Binary Alloy Phase Diagram*, ASM, Metals Park, Ohio, 1990.
- [29] P. Villars, L.D. Calvert, in: *Pearson's Handbook of Crystallographic Data for Intermetallic Phases*, ASM, Metals Park, OH, 1991.
- [30] L. Akselrud, Yu. Grin, WinCSD: software package for crystallographic calculations (Version 4), *J. Appl. Cryst.* 47, 803 (2014).
- [31] T. Roisnel, J. Rodriguez-Carvajal, WinPLOTR: a Windows tool for powder diffraction patterns analysis. *Mater. Sci. Forum* 378–381, 118 (2001).
- [32] M. Francois, G. Venturini, B. Malaman, B. Roques, *J. less-Common Met.* 160, 197 (1990).
- [33] R.V. Skolozdra, V.M. Mandzyk, L.G. Aksel'rud, *Sov. Phys. Crystallogr. (Engl. Transl.)* 26, 272 (1981).
- [34] M. Ruck, G. Portish, H.G. Schlager, M. Sieck, H. Löhniessen, *Acta Crystallogr. B49* (1993) 936–941.
- [35] C.P. Sebastian, C. Fehse, H. Eckert, R.D. Hoffmann, R. Pottgen, *Solid State Sci.* 8(11), 1386 (2006).
- [36] J.P. Maehlen, M. Stange, V.A. Yartys', R.G. Delaplane, *J. Alloys Compd.* 404, 112 (2005).
- [37] J.V. Pacheco, K. Yvon, E. Gratz, Z. Kristallogr. 213, 510 (1998).
- [38] S. Baran, V. Ivanov, J. Leciejewicz, N. Stusser, A. Szytula, A. Zygmunt, Y.F. Ding, *J. Alloys Compd.* 257, 5 (1997).
- [39] R. Pottgen, *J. Alloys Compd.* 243, L1 (1996).
- [40] K. Katon, T. Takabatake, A. Minami, I. Oguro, H. Sawa, *J. Alloys Compd.* 261, 32 (1997).
- [41] F. Yang, J.P. Kuang, J. Li, E. Brueck, H. Nakotte, F.R. de Boer, X. Wu, Z. Li, Y. Wang, *J. Appl. Phys.* 69(8), 4705 (1991).

Л.П. Ромака<sup>1</sup>, І.М. Романів<sup>1</sup>, В.В. Ромака<sup>2</sup>, М.Б. Коник<sup>1</sup>,  
А.М. Горинь<sup>1</sup>, Ю.В. Стадник<sup>1</sup>

## Ізотермічний переріз потрійної системи Ho–Cu–Sn при 670 К

<sup>1</sup>Львівський національний університет ім. І.Франка, вул. Кирила і Мефодія, 6, Львів, 79005, Україна,

<sup>2</sup>Національний університет “Львівська політехніка”, вул. Устияновича, 5, 79013 Львів, Україна

Взаємодія компонентів у потрійній системі Ho–Cu–Sn досліджена за температури 670 К в повному концентраційному інтервалі методами рентгенівської дифракції і рентгеноспектрального аналізу. При 670 К в системі утворюються чотири тернарні сполуки: HoCuSn (структурний тип LiGaGe, просторова група  $P6_3mc$ ), Ho<sub>3</sub>Cu<sub>4</sub>Sn<sub>4</sub> (структурний тип Gd<sub>3</sub>Cu<sub>4</sub>Ge<sub>4</sub>, просторова група  $Immm$ ), HoCu<sub>5</sub>Sn (структурний тип CeCu<sub>5</sub>Au, просторова група  $Pnma$ ) і Ho<sub>1.9</sub>Cu<sub>9.2</sub>Sn<sub>2.8</sub> (структурний тип Dy<sub>1.9</sub>Cu<sub>9.2</sub>Sn<sub>2.8</sub>, просторова група  $P6_3/mmc$ ). Встановлено утворення твердого розчину включення на основі бінарної сполуки HoSn<sub>2</sub> (структурний тип ZrSi<sub>2</sub>) до вмісту 5 ат. % Cu.

**Ключові слова:** інтерметаліди; фазові діаграми; рентгенівська дифракція; кристалічна структура.